BJA

British Journal of Anaesthesia, 128 (1): 159–173 (2022)

doi: 10.1016/j.bja.2021.10.020
Advance Access Publication Date: 26 November 2021
Pain

Role of primary sensory neurone cannabinoid type-1 receptors in pain and the analgesic effects of the peripherally acting agonist CB-13 in mice

Neil C. Ford[1,†], Awinita Barpujari[1,†], Shao-Qiu He[1], Qian Huang[1], Chi Zhang[1], Xinzhong Dong[2,3,4,5,6], Yun Guan[1,3,**] and Srinivasa N. Raja[1,2,*]

[1]Division of Pain Medicine, Department of Anesthesiology and Critical Care Medicine, Johns Hopkins University School of Medicine, Baltimore, MD, USA, [2]Department of Neurology, Johns Hopkins University School of Medicine, Baltimore, MD, USA, [3]Department of Neurological Surgery, Johns Hopkins University School of Medicine, Baltimore, MD, USA, [4]Solomon H. Snyder Department of Neuroscience, Johns Hopkins University School of Medicine, Baltimore, MD, USA, [5]Department of Dermatology, Johns Hopkins University School of Medicine, Baltimore, MD, USA and [6]Howard Hughes Medical Institute, Johns Hopkins University School of Medicine, Baltimore, MD, USA

**Corresponding author. E-mails: yguan1@jhmi.edu, sraja2@jhmi.edu

[†]N.C. Ford and A. Barpujari contributed equally to the study.

Abstract

Background: Cannabinoid type-1 receptors (CB_1Rs) are expressed in primary sensory neurones, but their role in pain modulation remains unclear.
Methods: We produced *Pirt*-CB_1R conditional knockout (cKO) mice to delete CB_1Rs in primary sensory neurones selectively, and used behavioural, pharmacological, and electrophysiological approaches to examine the influence of peripheral CB_1R signalling on nociceptive and inflammatory pain.
Results: Conditional knockout of *Pirt*-CB_1R did not alter mechanical or heat nociceptive thresholds, complete Freund adjuvant-induced inflammation, or heat hyperalgesia *in vivo*. The intrinsic membrane properties of small-diameter dorsal root ganglion neurones were also comparable between cKO and wild-type mice. Systemic administration of CB-13, a peripherally restricted CB_1/CB_2R dual agonist (5 mg kg^{-1}), inhibited nociceptive pain and complete Freund adjuvant-induced inflammatory pain. These effects of CB-13 were diminished in *Pirt*-CB_1R cKO mice. In small-diameter neurones from wild-type mice, CB-13 concentration-dependently inhibited high-voltage activated calcium current ($HVA\text{-}I_{Ca}$) and induced a rightward shift of the channel open probability curve. The effects of CB-13 were significantly attenuated by AM6545 (a CB_1R antagonist) and *Pirt*-CB_1R cKO.
Conclusion: CB_1R signalling in primary sensory neurones did not inhibit nociceptive or inflammatory pain, or the intrinsic excitability of nociceptive neurones. However, peripheral CB_1Rs are important for the analgesic effects of systemically administered CB-13. In addition, $HVA\text{-}I_{Ca}$ inhibition appears to be a key ionic mechanism for CB-13-induced pain inhibition. Thus, peripherally restricted CB_1R agonists could have utility for pain treatment.

Keywords: cannabinoid receptor; conditional knockout; dorsal root ganglion; high-voltage activated calcium current; inflammation; pain

Received: 30 June 2021; **Accepted:** 14 October 2021

Editor's key points

- Cannabinoids have been proposed as clinical analgesics, and cannabinoid type-1 receptors (CB_1Rs) are expressed in primary sensory neurones, but their role in pain modulation remains unclear.
- Selective knockout of CB_1Rs in primary sensory neurones did not alter mechanical or thermal nocifensive responses or intrinsic membrane properties, but reduced analgesia by the peripherally restricted CB_1R/CB_2R dual agonist CB-13.
- CB-13 concentration-dependently inhibited calcium currents in small-diameter dorsal root ganglion neurones, which provides a potential mechanism for its analgesic effects.
- Peripherally restricted CB1R agonists provide a translational approach to non-opioid analgesia without central cannabinoid side-effects.

Primary sensory neurones of the dorsal root ganglion (DRG) represent the major conduit through which peripheral sensory information, including noxious inputs, is transmitted to the spinal cord.[1,2] About 20% of adults across the USA and Europe suffer from chronic pain,[3,4] which leads to hundreds of billions of dollars in economic and societal costs.[5,6] Pharmacologic treatments that target mu-opioid receptors (MORs) have an unfavourable risk/benefit balance and significant limitations owing to central adverse effects.[7,8] Hence, interest has been growing in finding effective non-opioid pharmacologic targets for pain management.

The endocannabinoid system is a promising pharmacological target for new pain management strategies[9]; in particular, development of peripherally acting cannabinoid receptor agonists[10] may circumvent negative central effects and increase therapeutic viability. The cannabinoid type-1 receptor (CB_1R) is highly expressed in neurones of pain-related regions in the central and peripheral nervous systems,[11] including in the DRG.[12,13] Yet, the roles of peripheral CB_1R signalling in various pain conditions are only partially known, and previous findings have been contradictory. Several studies have shown a tonic peripheral endocannabinergic inhibition of nociceptive pain and inflammatory pain,[13,14] whereas others support a pro-nociceptive influence or no influence at all.[15,16] To ascertain whether endogenous CB_1R signalling in DRG neurones tonically modulates nociceptive pain, inflammatory pain, and intrinsic excitability of DRG neurones, we developed *Pirt*-CB_1R conditional knockout (cKO) mice for animal behavioural, pharmacological, and electrophysiological investigations. In *Pirt*-CB_1R cKO mice, CB_1R expression is selectively deleted in most DRG and trigeminal ganglion neurones because *Cre* recombinase is controlled by the *Pirt* promoter, which is expressed exclusively in >80% of primary sensory neurones, but not in any other cell type.[17]

In addition to endocannabinoids, synthesised CB_1R agonists inhibit small-diameter DRG neurones that are mostly nociceptive.[18] CB-13 is a potent CB_1/CB_2R dual agonist with limited brain penetration that may attenuate neuropathic mechanical hypersensitivity.[10,19] The ionic mechanisms of exogenous CB_1R agonist-induced neuronal inhibition may involve various ion channels and receptors, including high-voltage activated (HVA) calcium channels, TRPV1, acid-sensing ion channels, and inward-rectifying potassium channels.[20–23] Yet, much of the current evidence was gathered from recordings in heterologous systems rather than in native DRG neurones. Accordingly, we examined the effects of systemic CB-13 administration on nociceptive and inflammatory pain and determined the contribution of CB_1R and ionic mechanisms in DRG neurones to CB-13-induced pain inhibition.

Methods

Animals

Molecular experiments used 3–6-month-old wild-type (WT) mice (C57BL/6J; The Jackson Laboratory, Bar Harbor, ME, USA) and *Pirt*-$Cre^{+/-}$;$CB_1^{fl/fl}$ (*Pirt*-CB_1R cKO, or CB_1R cKO) mice. Behavioural experiments were conducted with adult $CB_1^{fl/fl}$ ($CB_1^{fl/fl}$ WT), CB_1R cKO, and *Pirt*-$Cre^{+/-}$;$Oprm^{fl/fl}$ (MOR cKO) mice. DRG for electrophysiological tests were harvested from $CB_1^{fl/fl}$ WT and CB_1R cKO mice (3–5 weeks old) of both sexes. Experiments were approved by the Institutional Animal Care and Use Committee, consistent with the National Institutes of Health (NIH) Guide for the Care and Use of Laboratory Animals.

Analysis of genomic DNA

Polymerase chain reaction (PCR) was used to detect the presence of $CB_1^{fl/fl}$ and *Pirt*-$Cre^{+/-}$ alleles in genomic DNA, using the following primer sequences: CB_1R: 5′-GCTGTCTCTGGTCC TCTTAAA-3′ (forward) and 5′-GGTGTCACCTCTGAAAACAGA-3′ (reverse); *Pirt-Cre:* 5′-ATCCGTAACCTGGATAGTGAA-3′ (*Cre* forward), 5′-CAACTTTGTGGTACCCGAAG-3′ (*Pirt* forward), and 5′-TCCCTGGGACTCATGATGCT-3′ (*Pirt* reverse).

Conditional knockout of CB_1R

Cre/*LoxP* recombination was used to generate *Pirt*-CB_1R cKO mice in which CB_1Rs were deleted specifically from most of primary sensory neurones. *Pirt*-Cre mice were provided by Xinzhong Dong (Johns Hopkins University, Baltimore, MD, USA), and $CB_1^{fl/fl}$ mice by George Kunos (NIH, Bethesda, MD, USA) and Elisabeth Glowatzki (Johns Hopkins University). Each mouse line was backcrossed to the C57BL/6J background. Owing to the disruption of the *Pirt* gene in homozygous *Pirt*-$Cre^{+/+}$ mice, which has been shown to alter TRPV1 functionality,[17] *Pirt*-$Cre^{+/-}$ mice were crossed with $CB1^{fl/fl}$ mice to generate the CB_1R cKO mice (Fig. 1a). *Pirt*-$Cre^{+/-}$ mice have no known phenotype that affects receptor function or interpretation of behavioural results, and have been used to generate other cKO mice used in studies of pain behaviour.[24,25] The control WT mice expressed only $CB_1^{fl/fl}$. *Pirt*-MOR cKO mice, in which MORs were deleted specifically from primary sensory neurones, were similarly generated to be used in pharmacologic studies to examine whether efficacy of pain inhibition by systemic CB-13 is influenced by endogenous MOR signalling in DRG neurones.

Immunohistochemistry

Cryosections of lumbar DRGs (4% paraformaldehyde fixed) were immunostained with rabbit anti-CB_1R antibody (1:200; 10006590; Cayman, Ann Arbor, MI, USA), with Alexa 488-conjugated goat antibody to rabbit (A-11008; Thermo Fisher Scientific, Waltham, MA, USA) as the secondary antibody (1:100). Raw confocal (TIFF) images (LSM 700; Zeiss, White Plains, NY, USA) were analysed with Fiji (NIH). The total

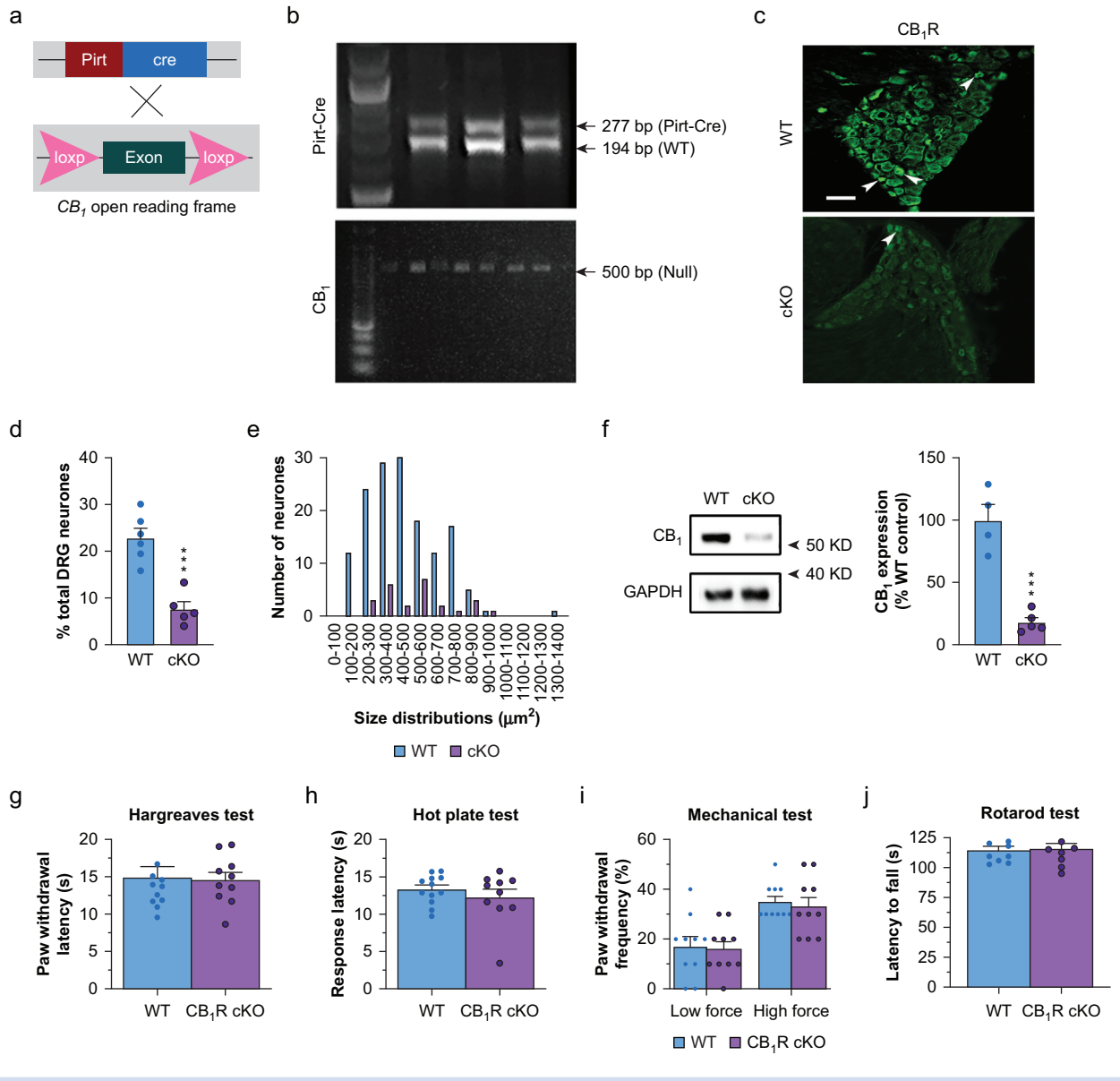

Fig 1. Pirt-Cre conditional knockout (cKO) of CB1R in dorsal root ganglion (DRG) neurones does not affect nociceptive thresholds or locomotor function. (a) Strategy for generating CB1R cKO mice. Pirt-Cre$^{+/-}$ mice and CB$_1^{fl/fl}$ mice were intercrossed to delete CB1 expression exclusively in most primary sensory neurones. (b) Representative images of ethidium bromide-stained agarose gels show PCR genotyping of Pirt-Cre (top) and CB1 (bottom) from tail snip tissue samples. The upper band (277 bp) in the Pirt-Cre panel indicates the Pirt-Cre^{+} allele, and the lower band (194 bp) indicates the WT allele (Pirt gene without Cre [Pirt-Cre^{-}]). The single band (500 bp) in the CB1 panel indicates the null gene (floxed allele [ΔCB$_1^{fl/fl}$]). (c) Representative images of immunofluorescence-stained DRG sections. A subset of neurones were stained with the CB1R antibody in WT mice but the staining was much less in CB1R cKO mice. Scale bar: 50 μm. (d) Quantification of CB1R-positive neurones in the L4–L6 DRGs of each group (***P=0.0003, unpaired *t*-test, *n*=5–6 mice/group). (e) Size distribution of CB1R-positive neurones, which are predominantly small-diameter (area ≤600 μm^2) in WT mice. (f) Left panel, representative Western blot images of CB1R protein expression in the DRGs of WT and CB1R cKO mice. Right panel, quantification of CB1R protein levels (***P=0.0002, unpaired *t*-test, *n*=4–5 mice/group). (g, h) CB1R cKO and WT mice displayed similar withdrawal latency of the hind paw in response to radiant heat stimulus (g; P=0.85, Welch's *t*-test, *n*=10/group, five/sex in each group) and comparable response latencies in the hot plate test (h; P=0.42, Welch's *t*-test). (i) CB1R cKO and WT mice displayed similar paw withdrawal frequency ($F_{1,36}$=0.023, P=0.88, two-way ANOVA) to low force (0.07 g; P>0.99) and high force (0.4 g; P>0.99, Bonferroni's post-test) mechanical stimulation with von Frey monofilaments. (j) Latency to fall during the rotarod test was comparable between WT and CB1R cKO mice (P=0.89, Welch's *t*-test). Data are shown as mean (standard error of the mean). CB1R, cannabinoid type-1 receptor; cKO, conditional knockout; PCR, polymerase chain reaction; WT, wild-type; ANOVA, analysis of variance.

number of neurones in each section was determined by counting both labelled and unlabelled cell bodies. Positively stained neurones had clear stomata and an increase in fluorescence intensity ≥30% of background. To quantify the neuronal cross-sectional area of DRG neurones, cells were identified by morphology with a clearly defined, dark, condensed nucleolus. Positively stained cells were chosen for cross-sectional area measurement. The somata of the labelled cells were traced manually with the Fiji 'Freehand selection' tool and the areas were measured. Tissues from different groups were processed together.

Western immunoblotting

Mouse DRGs were harvested and the tissues were lysed in radioimmunoprecipitation assay (RIPA) buffer (Sigma, St. Louis, MO, USA) containing protease/phosphatase inhibitor cocktail (Cell Signaling Technology, Boston, MA, USA). A standard bicinchoninic acid protein assay (Thermo Fisher Scientific) was used to determine protein concentration of RIPA lysates. Samples (20 μg) were separated on a 4–12% Bis-Tris Plus gel (Thermo Fisher Scientific) and then transferred onto a polyvinylidene difluoride membrane (Thermo Fisher Scientific). Immunoreactivity was detected by enhanced chemiluminescence (ECL; Bio-Rad, Hercules, CA, USA) after incubating the membranes with the indicated primary antibody (4°C, overnight). We used primary antibodies against CB1 receptor (1:1000; Cayman) and CB2 receptor (1:1000; Cayman). Glyceraldehyde 3-phosphate dehydrogenase (GAPDH, 1:100 000; Millipore, Darmstadt, Germany) was used as an internal control for protein loading. ImageJ (ImageJ 1.46r) was used to quantify the intensity of immunoreactive bands of interest on autoradiograms.

Inflammatory pain model

Under isoflurane (Sigma, 2%, mixed in 2.5 L min^{-1} oxygen) anaesthesia, 20 μl of 1 mg ml^{-1} complete Freund's adjuvant (CFA; Sigma-Aldrich, St. Louis, MO, USA) was injected into the intra-plantar region of the left hind paw. Paw oedema and heat hypersensitivity were assessed at 24 and 72 h after injection. The dorsoventral paw thickness was measured with a digital calliper at the metatarsophalangeal border.

Behavioural pain tests

Before behavioural testing, animals were subjected to a 30-min acclimatisation period inside the testing room with the experimenter, to minimise the effects of the testing environment. All testing occurred between 09:00 and 17:00. Animals were randomised to treatment groups, and investigators were blinded to treatment. Sample sizes were determined based on similar protocols in previous studies.[24,26]

Mechanical hypersensitivity was evaluated by measuring paw withdrawal frequency (PWF) to von Frey filament stimulation.[27] Briefly, low-force (0.07 g) and high-force (0.45 g) von Frey monofilaments (Stoelting Co., Wood Dale, IL, USA) were applied to the mid-plantar area of each hind paw 10 times (with 1–2 s intervals). Vertical elevation of the paw, licking, or both were considered positive withdrawal responses.

Heat nociception was examined in the hot plate test (55°C; Ugo Basile, Varese, Italy), and response latencies were recorded. Nocifensive behaviours included forepaw or hind paw withdrawal or licking, stamping, leaning posture, and jumping. The Hargreaves test was also used to assess heat hypersensitivity. Animals were placed in Plexiglas chambers positioned on a heated glass floor (30°C). Radiant heat was applied to the plantar surface of the hind paw, and paw withdrawal latency (PWL) was measured using an automatic plantar stimulator meter (IITC model 390; IITC Life Sciences, Woodland Hills, CA, USA). Both procedures were repeated three times (5 min intervals) and data were averaged for analysis. A cut-off time of 30 s was used to prevent sensitisation and tissue damage. Behavioural results were analysed together after initial sex comparisons of nociceptive thresholds showed that there were no significant differences in the tests that would be used in subsequent pain model/drug testing (Supplementary Fig. S2).

Motor function evaluation

Locomotor activity was evaluated with open field tests. After a 30-min acclimatisation period inside the testing room, one mouse per trial was placed in the corner of a Plexiglass arena (50 × 50 × 38 cm) equipped with a video tracking system (SMART 3; Panlab Harvard Apparatus; Barcelona, Spain). Mice were then allowed to freely explore for 10 min. The distance that the mice travelled was tracked and recorded by the SMART 3 software. The testing arena was cleaned with 70% ethanol before and after each trial. To assess the effects of CB-13 administration on locomotive activity, after the mice were acclimated to the testing room, CB-13 (5 mg kg^{-1}, s.c.) or vehicle was administered between the shoulders under isoflurane anaesthesia. Mice were then allowed to recover from anaesthesia in their home cage for 30 min before open field testing.

Motor coordination, ataxia, and equilibrium were evaluated with rotarod tests (Ugo Basile). Before training or testing sessions, animals were first acclimatised to the testing room for 30 min. For training sessions (three times, 10 min intervals), mice were placed in separate lanes on a rod rotating at 5 rpm for 60 s. Animals unable to remain on the rod for 60 s were excluded from further study. For testing, animals were placed on a rod rotating at 4 rpm and then accelerated to 40 rpm over 300 s. The trial began at the start of acceleration and ended when the animal fell from the rod. Fall latencies were recorded, and the average of three trials was used for analysis. To assess the effects of CB-13 administration on motor coordination, mice were first acclimatised to the testing room for 30 min before both the training and testing sessions. Training sessions were run as above. For testing sessions, under isofluorane anaesthesia, CB-13 (5 mg kg^{-1}, s.c.) or vehicle was administered between the shoulders. Mice were then allowed to recover from anaesthesia in their home cage for 30 min before rotarod testing.

Dorsal root ganglion neuronal culture

Bilateral L4–L6 DRGs were collected from deeply anaesthetised (3% isoflurane) WT and CB_1R cKO mice, and placed into fresh, ice-cold DH10 media consisting of Dulbecco's modified Eagle's medium (DMEM)/F-12 supplemented with 10% fetal bovine serum (no dimethyl sulfoxide [DMSO]) and 1% penicillin/streptomycin (~1.5 ml per animal) and washed in Hanks balanced salt solution (HBSS; Gibco, Dublin, Ireland). Then, an enzyme solution containing 3.55 mg ml^{-1} dispase (Worthington Biochemicals, Lakewood, NJ, USA) and 1.65 mg ml^{-1} collagenase type I (Gibco) in HBSS without Ca^{2+} and Mg^{2+}

was applied. Cells were incubated at 37°C for 45–60 min with gentle shaking/rotation every 10 min. After trituration, the cell suspension was strained through a 40 μm mesh (Sigma-Aldrich) and centrifuged (5 min, 4°C, 58 *g*). Cells were resuspended in DH10 medium containing nerve growth factor (NGF; 20 ng ml^{-1}; Upstate Biotechnology, Lake Placid, NY, USA) and glial cell line derived neurotrophic factor (GDNF; 50 ng ml^{-1}; Upstate Biotechnology) then plated on coverslips freshly coated with poly-D-lysine (100 μg ml^{-1}; Biomedical Technologies) and laminin (100 μg ml^{-1}). Cultures were incubated at 37°C in 5% CO_2 for ~48 h before electrophysiological recordings.

Whole-cell patch-clamp recording

Patch-clamp electrodes were constructed from single-filament borosilicate glass (1.5 mm o.d., 0.84 mm i.d.; World Precision Instruments, Sarasota, FL, USA; impedance: 2–4 MΩ) and formed seal resistances ≥1 GΩ. All recordings were obtained at room temperature. All solution/drug perfusions were delivered at a rate of 1–2 ml min^{-1}.

For intrinsic excitability recordings under current clamp conditions, neurones were perfused with an oxygenated solution of (in mM) 140 NaCl, 4 KCl, 2 $MgCl_2$, 2 $CaCl_2$, 10 4-(2-hydroxyethyl)-1-piperazineethanesulfonic acid (HEPES), and 10 glucose (pH=7.4 adjusted with NaOH; ~305–310 mOsm) adjusted with sucrose, measured by an osmometer (Vapro 5600; Wescor, Logan, UT, USA). Junction potential differences between internal and external solutions (15.7 mV; junction potential calculator; Clampex software, Molecular Devices, San Jose, CA, USA) were corrected for. The internal solution was composed of (in mM) 135 K-gluconate, 10 KCl, 10 HEPES, 2 Na_2ATP, 0.4 Na_2GTP, and 1 $MgCl_2$ (pH=7.4 with KOH; ~300–305 mOsm).

For HVA-I_{Ca} recording under voltage-clamp conditions, neurones were perfused with an oxygenated solution consisting of (in mM) 130 N-methyl-D-glucamine chloride (NMDG-Cl; solution of 130 mM NMDG pH balanced to 7.4 with HCl), 5 $BaCl_2$, 1 $MgCl_2$, 10 HEPES, and 10 glucose (pH=7.4 adjusted with 1 M NMDG; ~310–315 mOsm adjusted with sucrose). Junction potential differences between the internal and external solutions were not adjusted. The internal solution was composed of (in mM) 140 TEA-Cl, 10 ethylene glycol-bis(β-aminoethyl ether)-*N*,*N*,*N*′,*N*′-tetraacetic acid (EGTA), 1 $MgCl_2$, 10 HEPES, 0.5 Na_2GTP, and 3 Na_2ATP (pH=7.4 with 1 M NMDG; ~300–305 mOsm).

All recordings were filtered at 4 kHz with a −3 dB, four-pole, low-pass Bessel filter, sampled at a rate of 20 kHz, and stored on a personal computer (Dell) using pClamp 11 and a digitiser (Digidata 1550B; Molecular Devices). Currents were digitally filtered offline by using a low-pass Gaussian filter with a −3 dB cut-off set to 2 kHz (Clampfit software; pClamp 11, Molecular Devices).

Intrinsic excitability

After whole-cell configuration was established, a 5 min equilibration period was allowed before the spontaneous activity of the neurone was recorded for 2 min from V_{rest}. Rheobase was measured by injecting a series of square-wave current steps via the patch electrode (500 ms, 10 pA steps; starting at −40 pA) until a single action potential (AP) was generated. AP threshold (mV), AP amplitude (mV), AP half-width (ms), and input resistance (MΩ) were then measured. AP trains in response to a prolonged current application via the patch electrode (1×, 2×, and 3× rheobase intensity; 1 s) were then recorded. Both the number of APs and the instantaneous frequency of APs (Inst. Freq [Hz]=mean interspike interval^{-1} [ms]) generated by each stimulus intensity were computed.

High voltage-activated calcium current recording

Under whole-cell configuration, series resistance was maintained at <20 MΩ under voltage-clamp conditions. For examination of HVA-I_{Ca} current–voltage (I–V) relationships and channel open probabilities after a 5 min equilibration period, 25 ms depolarising square wave voltage steps were delivered via the patch electrode (−70 to +40 mV, 10 mV step).[28,29]

Protocols used to evoke low-voltage-activated (LVA) and HVA currents were based on prior studies.[28,29] Briefly, with neurones held at −80 mV, once every 10 s a +40 mV pulse was applied via the patch electrode for 20 ms to activate LVA Ca^{2+} channels. The holding voltage was then set to −60 mV for 20 ms followed by a +50 mV step for 20 ms to evoke HVA-I_{Ca}. After recording 1 min of baseline HVA-I_{Ca}, CB-13 (1–10 nM), vehicle, CB-13 (10 nM) + AM6545 (10 nM), or CB-13 (10 nM) + AM630 (100 nM) was delivered by bath application using a perfusion system (VC-6; Warner Instruments, Hamden, CT, USA) for 2 min, followed by 15 min of washout.

Analysis of channel open probabilities

The current–voltage relationship (I–V curve) was determined by plotting normalised peak HVA-I_{Ca} amplitudes at each test voltage (−70 to +40 mV). The voltage dependency of channel open probabilities was determined by plotting normalised tail currents as a function of test voltages, which were then fitted with a Boltzmann equation for channel open probabilities:

$$P(V) = P_{min} + \frac{P_{max} - P_{min}}{1 + e^{\frac{V - V_{half}}{k}}},$$

where $P(V)$ represents the channel open probability as a function of membrane potential; P_{min} and P_{max} are the minimum and maximum open probabilities, respectively; V_{half} is the voltage at 50% maximum current; and k is the default slope value.

Drugs

CB-13 (1-naphthalenyl[4-(pentyloxy)-1-naphthalenyl]methanone; Tocris, Bristol, UK), a dual agonist of CB_1R (EC_{50}=6.1 nM) and CB_2R (EC_{50}=27.9 nM), was diluted with DMSO followed by normal saline, and injected subcutaneously (5 mg kg^{-1}) or diluted with NMDG-Cl solution for electrophysiological testing (1–10 nM). AM6545 (5-[4-(4-cyano-1-butyn-1-yl)phenyl]-1-(2,4-dichlorophenyl)-N-(1,1-dioxido-4-thiomorpholinyl)-4-methyl-1H-pyrazole-3-carboxamide; Sigma), a high-affinity CB_1R antagonist (K_i=3.1 nM), and AM630 (6-iodo-2-methyl-1-2-(4-morpholinyl)ethyl-1*H*-indol-3-yl(4-methoxyphenyl)methanone; Sigma), a CB_2R inverse agonist (K_i=31.2 nM), were dissolved in DMSO to stock concentration, and in NMDG-Cl solution for electrophysiological tests (AM6545: 10 nM; AM630: 100 nM). All drug solutions were freshly prepared before use,

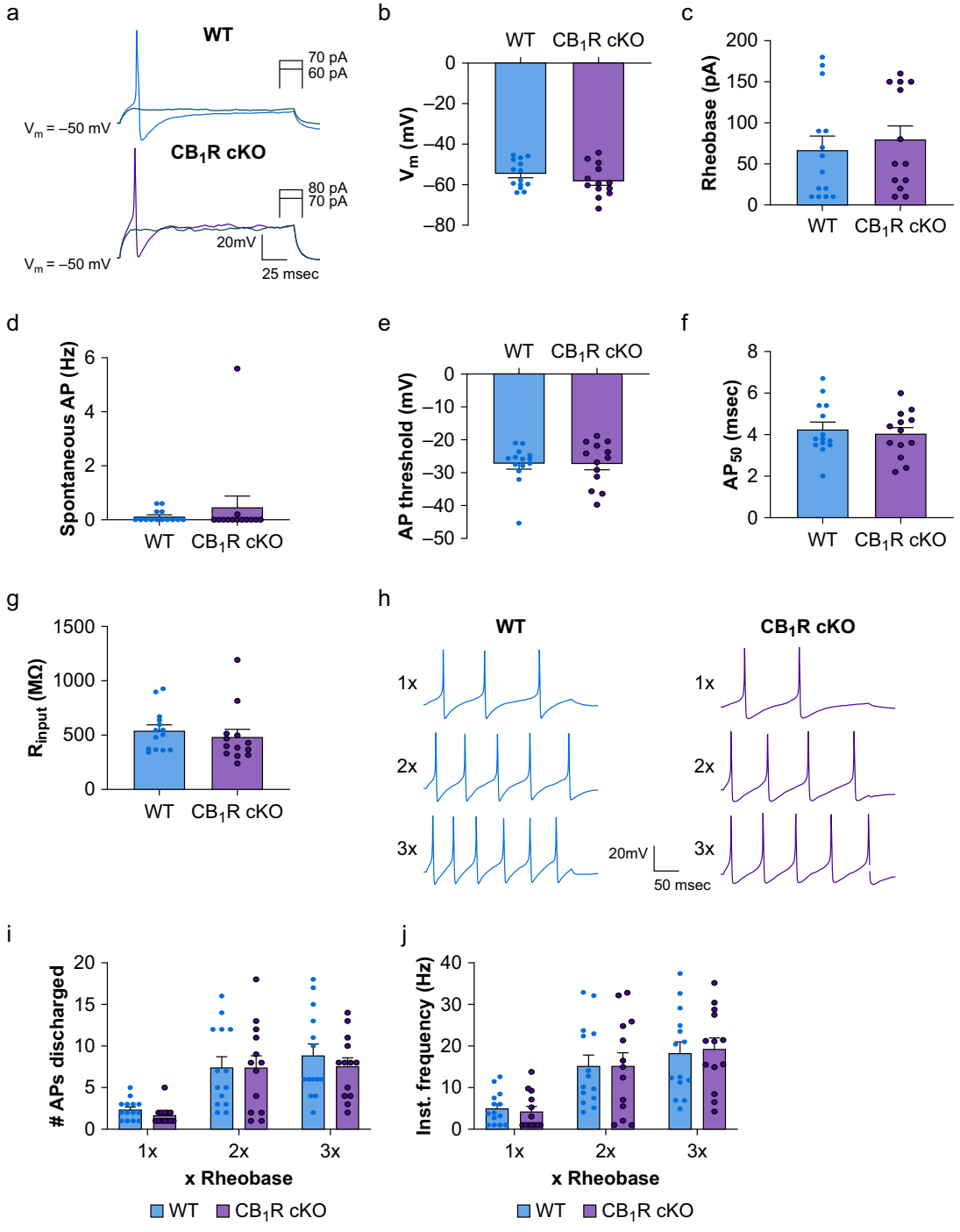

Fig 2. The intrinsic membrane properties of small-diameter dorsal root ganglion (DRG) neurones are not affected by CB1R conditional knockout. (a) Representative traces of rheobase levels of small-diameter DRG neurones from wild-type (WT) and CB1R cKO mice under current-clamp conditions. The electrophysiological parameters shown in panels b–g did not differ significantly between the WT and CB1R cKO groups (n=13–14 neurones/group, four mice/sex). (b) Resting membrane potentials (P=0.26). (c) Rheobase levels (P=0.62). (d) Rate of spontaneous action potential (AP) discharge (P=0.76). (e) AP threshold (P=0.97). (f) AP half-width (AP50; P=0.61). (G) Input resistance (R_{input}; P=0.48). (h) Representative traces of AP trains evoked by current stimulation (1×, 2×, 3× rheobase intensity) of small-diameter neurones from WT and CB1R cKO mice. (i, j) The number of APs generated (1×: P=0.89, 2×: P=0.98, 3×: P=0.78) and the instantaneous frequency (1×: P=0.99, 2×: P=0.99, 3×: P=0.98) of AP trains discharged by DRG neurones did not differ between WT (n=14 neurones) and CB1R cKO mice (n=13 neurones) across stimulation intensities. (b–g): unpaired t-test; (i, j): two-way mixed-model ANOVA. Data are shown as mean (standard error of the mean). CB1R, cannabinoid type-1 receptor; cKO, conditional knockout; ANOVA, analysis of variance.

and concentrations used were determined by their EC_{50} based on preliminary concentration–effect analysis and previous studies.[26]

Statistical analysis

Data were subjected to normality tests (Shapiro–Wilk or Kolmogorov–Smirnov). Behavioural data with naïve animals were compared across genotypes with Welch's *t*-test or Mann–Whitney *U*-test. The time course of drug and pain model effects was assessed using repeated-measures or mixed-model two-way analysis of variance (ANOVA), with Bonferroni, or Holm–Sidak *post hoc* tests. The Greenhouse–Geisser correction was used to adjust for lack of sphericity in the repeated-measures ANOVA.

Current-clamp data were compared using unpaired *t*-tests. Data from voltage-clamp experiments involving drug/antagonist tests were compared using two-way repeated measures or mixed-model ANOVA with Holm–Sidak tests for multiple comparisons. Prism 9.0 (GraphPad Inc., San Diego, CA, USA) was used for statistical analyses. All tests were two-tailed, with *statistical significance set at* $P<0.05$. Data are presented as mean (standard error of the mean [SEM]).

Results

Nociceptive thresholds or locomotor function not affected by knockout of CB_1R in primary sensory neurones

We tested whether endogenous CB_1R signalling in DRG neurones tonically inhibits nociceptive sensitivity or affects locomotor function. Through *Pirt*-Cre/*LoxP*-mediated recombination, CB_1R expression was conditionally knocked out in a majority of DRG neurones in CB_1R cKO mice (Fig. 1a and b). The proportions of CB_1R-positive neurones (% of total neurones counted) were significantly reduced compared with those in WT mice (Fig. 1c and d; $t_9=5.64$, $P=0.0003$, unpaired *t*-test). Size distribution analysis showed that CB_1Rs were expressed predominantly in small- and medium-diameter ($\leq 600\ \mu m^2$) neurones in WT mice (Fig. 1e). CB_1 immunoreactivity of the central terminals within the spinal superficial dorsal horn (SDH) was also reduced in CB_1R cKO mice compared with WT (Supplementary Fig. S1b; $t_6=4.16$, $^*P=0.01$, Bonferroni's post-test).

By immunoblotting, CB_1 protein (50 kDa) levels were reduced in the DRG of CB_1R cKO mice (Fig. 1f; $t_7=6.87$, $^{***}P=0.0002$, unpaired *t*-test). In addition, CB_2 (40 kDa) protein levels were also reduced in CB_1R cKO mice (Supplementary Fig. S1a; $t_8=2.41$, $^*P=0.04$, unpaired *t*-test).

In behavioural studies, naive WT and CB_1R cKO mice responded to radiant heat stimulation with similar paw withdrawal latencies (Fig. 1g; $t_{19}=0.193$, $P=0.85$, Welch's *t*-test), and exhibited similar response latencies in the hot plate test (Fig. 1h; $t_{13}=0.835$, $P=0.42$, Welch's *t*-test). Paw withdrawal frequencies to punctate mechanical stimulation were also comparable between the two groups (Fig. 1i, 0.07 g: $t_{36}=0.215$, $P>0.99$; 0.4 g: $t_{36}=0.429$, $P>0.99$, Bonferroni's post-test). Motor coordination was similar in WT and CB_1R cKO mice as evidenced by comparable fall latencies in the rotarod test (Fig. 1j; $t_{13}=0.147$, $P=0.89$, Welch's *t*-test). Overall, there were no significant sex differences in mechanical thresholds or radiant heat thresholds (Supplementary Fig. S2a–c). However, there was a significant sex difference in response latencies to hot plate tests in CB_1R cKO mice (Supplementary Fig. S2d; $t_{16}=2.55$, $P=0.04$, Holm–Sidak post-test).

No effect of knockout of CB_1R on intrinsic membrane properties of small-diameter DRG neurones

To investigate whether constitutive activation of CB_1R modulates DRG neurone excitability, we compared the intrinsic excitability of small-diameter neurones in WT and CB_1R cKO mice. Patch-clamp recordings showed no significant difference in resting membrane potential (Fig. 2a and b; $t_{25}=1.16$, $P=0.26$; mean: WT, −54.8 [1.8] mV; cKO, −58.1 [2.2] mV), rheobase level (Fig. 2c; $t_{25}=0.51$, $P=0.62$; mean: WT, 64.2 [16.8] pA; cKO, 79.2 [17.0] pA), spontaneous AP discharge (Fig. 2d; $t_{25}=0.45$, $P=0.76$; mean: WT, 0.13 [0.06] Hz; cKO, 0.45 [0.43] Hz), AP threshold (Fig. 2e; $t_{25}=0.035$, $P=0.97$; mean: WT, −27.3 [1.6] mV; cKO, −27.2 [1.9] mV), AP half-width (Fig. 2f; $t_{25}=0.52$, $P=0.61$; mean: WT, 4.3 [0.3] ms; cKO, 4.02 [0.31] ms), or input resistance (Fig. 2g; $t_{25}=0.72$, $P=0.48$, unpaired *t*-test; mean: WT, 543 [51] MΩ; cKO, 482 [71] MΩ) between the two genotypes. Additionally, neurones in both groups discharged similar AP trains evoked by increasing stimulation intensities (1–3× rheobase). The number of APs (Fig. 2i and Supplementary Table S1; 1×: $t_{75}=0.43$, $P=0.89$; 2×: $t_{75}=0.029$, $P=0.98$; 3×: $t_{75}=0.86$, $P=0.78$) and the instantaneous frequency of APs (Fig. 2j and Supplementary Table S1; 1×: $t_{75}=0.22$, $P=0.99$; 2×: $t_{75}=0.001$, $P=0.99$; 3×: $t_{75}=0.31$, $P=0.98$) generated by WT and CB_1R cKO neurones in response to each stimulation intensity did not differ between the two groups (Supplementary Table S1).

CB-13 inhibition of nociceptive pain and inflammatory heat hyperalgesia reduced in CB_1R conditional knockout mice

Owing to potential functional interactions between CB_1Rs and MORs,[30,31] significant CB_1R-MOR interactions may alter CB-13 efficacy under conditions where MORs are absent in DRG neurones as endogenous MOR signalling and the resulting CB_1R interactions would be compromised. Accordingly, we examined systemic CB-13 effects on nociceptive pain and inflammatory heat hyperalgesia in *Pirt*-MOR cKO, *Pirt*-CB_1R cKO, and WT mice.

Systemic CB-13 administration (5 mg kg^{-1}; s.c.) increased PWL at 60 min after injection in both WT (Fig. 3a; $t_{52}=2.79$, $P<0.05$) and MOR cKO mice ($t_{52}=2.78$, $P<0.05$), but not in CB_1R cKO mice ($t_{52}=0.48$, $P>0.99$, Bonferroni's post-test). CB-13 also decreased PWF in WT (Fig. 3b; $t_{52}=3.9$, $P<0.001$) and MOR cKO mice ($t_{52}=4.38$, $P<0.001$), but not in CB_1R cKO mice ($t_{52}=0.78$, $P=0.88$, Bonferroni's post-test). Changes in PWL and PWF after CB-13 treatment were comparable between WT and MOR cKO mice. Thus, genetic deletion of CB_1Rs, but not MORs, in primary sensory neurones reduced the antinociceptive effects of CB-13.

We further investigated whether peripheral CB_1R signalling modulates the development of heat hyperalgesia and the analgesic effect of systemic CB-13 under inflammatory pain conditions. Intra-plantar injection of CFA (20 μL, 1 mg ml^{-1}) caused similar paw thickness increases in WT (Fig. 3c; $t_{29}=16.7$, $P<0.001$) and CB_1R cKO mice ($t_{29}=21.5$, $P<0.001$, Bonferroni's post-test). Ipsilateral PWLs were decreased to a similar level in WT (Fig. 3d; $t_{19}=9.5$, $P<0.001$) and CB_1R cKO

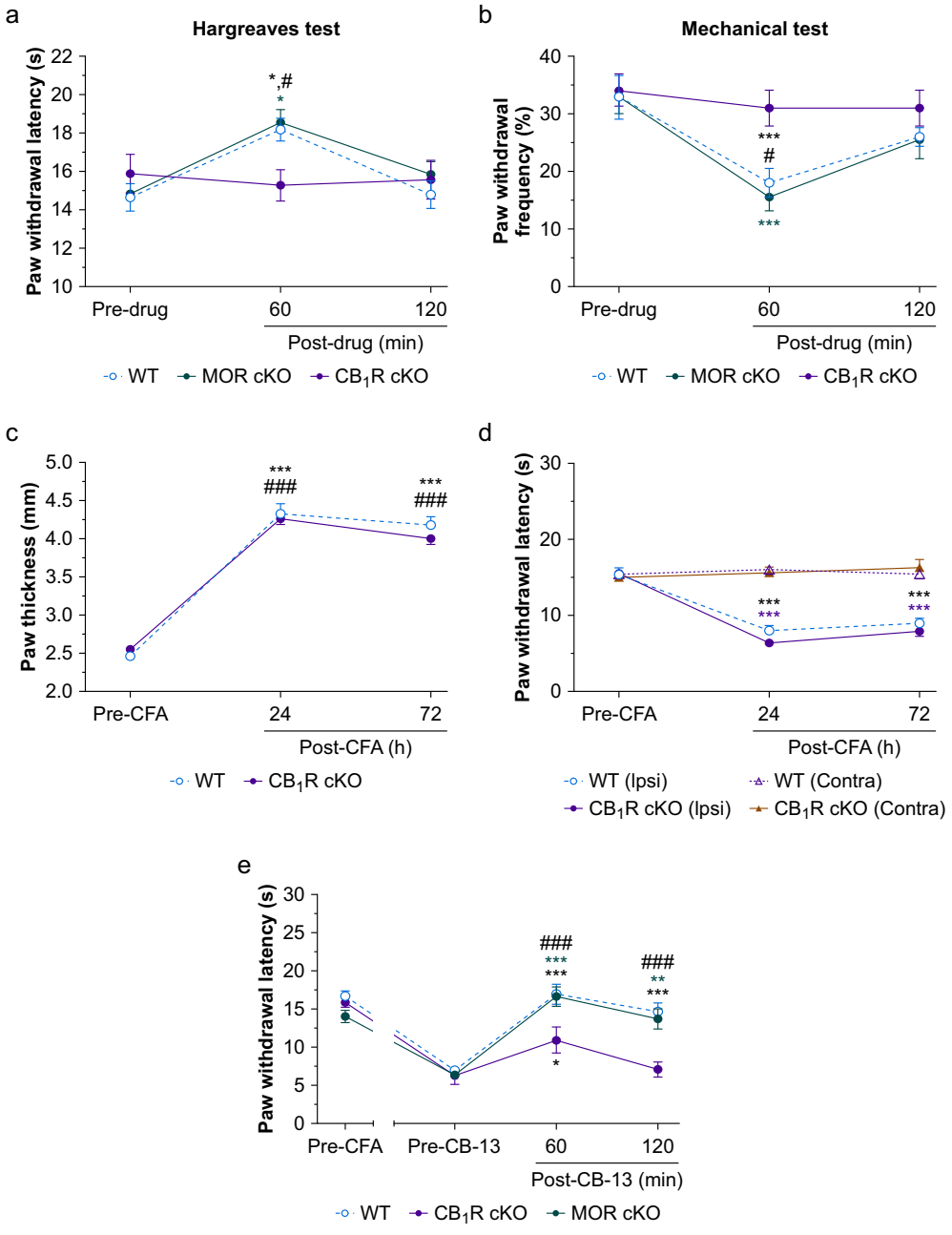

Fig 3. Systemic administration of CB-13 strongly inhibits nociceptive pain and inflammatory heat hypersensitivity in wild-type (WT) mice and in mice lacking peripheral mu-opioid receptors (MOR cKO) but weakly in CB1R cKO mice. (a) Systemic administration of CB-13 (5 mg kg^{-1}, s.c.) significantly increased paw withdrawal latency (PWL) to radiant heat stimulation in both WT and MOR cKO mice at 60 min, but not in CB1R cKO mice ($F_{2,52}$=5.23, P=0.009, two-way mixed-model ANOVA). *P<0.05 *vs* pre-drug, #P<0.05 *vs* CB1R cKO, Bonferroni's post-test. (b) CB-13 (5 mg kg–1, s.c.) significantly decreased paw withdrawal frequency (PWF) to high-force (0.4 g) mechanical stimulation at 60 min in both WT and MOR cKO mice, but not in CB1R cKO mice ($F_{2,52}$=13.89, P<0.001, two-way mixed model ANOVA). ***P<0.001 *vs* pre-drug; #P<0.05 *vs* CB1R cKO, Bonferroni's post-test (a, b: n=10/group, five/sex in each group). (c) Intraplantar injection of complete Freund's adjuvant (CFA; 20 µl, 1 mg ml^{-1}) similarly increased paw thickness in WT and CB1R cKO mice ($F_{2,114}$=393.7, P<0.001, two-way mixed model ANOVA). ***P<0.001 *vs* pre-CFA of WT, ###P<0.001 *vs* pre-CFA of CB1R cKO, n=30 mice/group, Bonferroni's post-test. (d) PWL to radiant heat stimulation was significantly decreased in the ipsilateral hind paw of both groups after intraplantar CFA injection ($F_{6,152}$=20.26, P<0.001, two-way mixed model ANOVA). ***P<0.001 *vs* pre-CFA, n=20 mice/group, 10/sex, Bonferroni's post-test. (e) Effects of systemic CB-13 (5 mg kg^{-1}, s.c.) on the ipsilateral PWL of mice at 72 h post-CFA ($F_{6,78}$=6.4, P<0.001, two-way mixed-model ANOVA). WT and CB1R cKO: n=10/group, five/sex; MOR cKO: n=9 mice. *P<0.05, **P<0.01, ***P<0.001 *vs* pre-drug values; ###P<0.001, WT and MOR cKO *vs* CB1R cKO, Bonferroni's post-test. Data are shown as mean (standard error of the mean). Ipsi, ipsilateral; Contra, contralateral; ANOVA, analysis of variance.

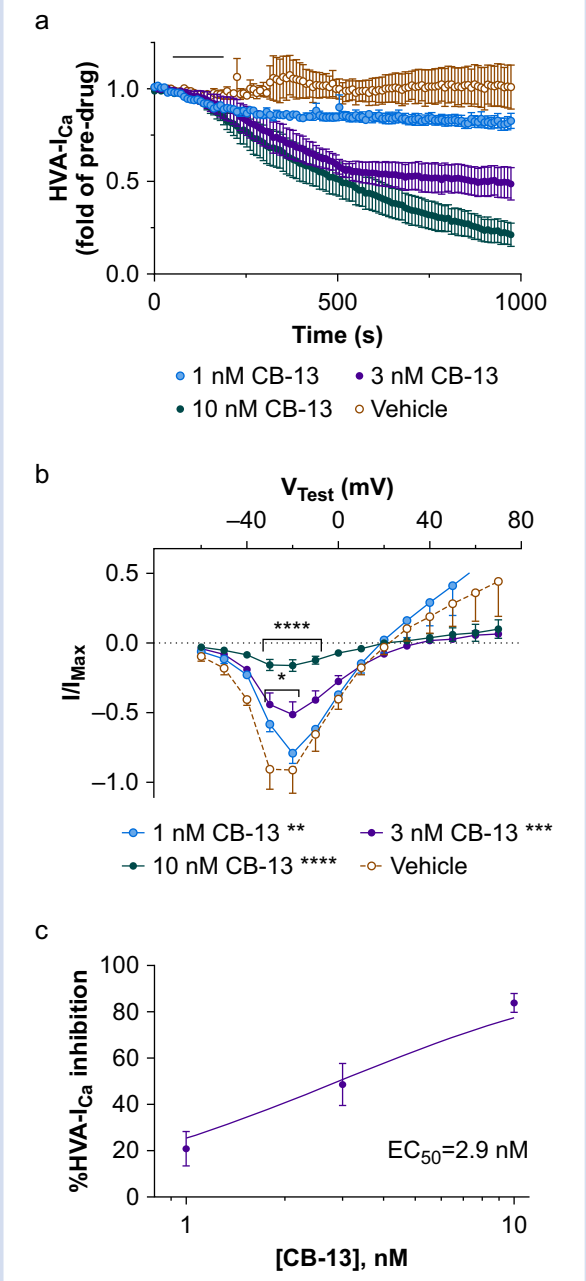

Fig 4. CB-13 inhibits high-voltage activated calcium currents (HVA-I_{Ca}) in small-diameter dorsal root ganglion (DRG) neurones from wild-type (WT) mice. (a) Bath application of CB-13 (horizontal black bar: 1, 3, and 10 nM) dose-dependently inhibited HVA-I_{Ca} in cultured small-diameter DRG neurones from WT mice ($P<0.0001$, two-way mixed-model ANOVA). $n=3–5$ neurones/group. (b) CB-13 (1–10 nM) also dose-dependently altered the current–voltage (I–V) relationship of HVA-I_{Ca} conductance ($F_{30,132}=6.2$, $P<0.0001$, two-way mixed model ANOVA) in WT mice. Increasing CB-13 concentration produced progressively larger reductions in HVA-I_{Ca} conductance (1 nM: **$P<0.01$; 3 nM: ***$P<0.001$; 10 nM: ****$P<0.0001$ compared with vehicle treatment, Holm–Sidak post-test). *$P<0.05$, ****$P<0.0001$ *vs* vehicle at corresponding test voltages, Holm–Sidak post-test. (c) Dose–response curve for the inhibitory effect of CB-13 on HVA-I_{Ca} (% HVA-I_{Ca} inhibition) in WT mice. I/I_{Max} values from $V_{Test}=-20$ mV at peak of drug inhibition compared with pre-drug values ($EC_{50}=2.9$ nM). ANOVA, analysis of variance.

mice ($t_{19}=15$, $P<0.001$, Bonferroni's post-test) at 72 h after CFA. Contralateral PWLs were not significantly changed (Fig. 3d). CB-13 (5 mg kg^{-1}; s.c.) increased PWLs in WT (Fig. 3e; $t_9=8.7$, $P<0.001$) and MOR cKO mice ($t_9=8.23$, $P<0.001$, Bonferroni's post-test) at both 60 and 120 min after drug injection compared with pre-drug. CB-13 only modestly increased PWL in CB_1R cKO mice ($t_9=3.5$, $P<0.05$, Bonferroni's post-test). Importantly, the increased PWLs in WT and MOR cKO mice at 60 and 120 min after CB-13 injection were greater than in CB_1R cKO mice (Fig. 3e; WT: $t_{104}=4.0$, $P<0.001$; MOR cKO: $t_{104}=3.7$, $P<0.001$, Bonferroni's post-test).

We verified that the CB-13 dose does not affect locomotion or motor coordination (Supplementary Fig. S3). There were no differences in total distance travelled in open field testing (Supplementary Fig. S3b; $t_9=0.35$, $P=0.74$, unpaired *t*-test) or mean latency to fall in rotarod tests (Supplementary Fig. S3c; $t_9=1.14$; $P=0.28$) following either systemic CB-13 (5 mg kg^{-1}, s.c.) administration or vehicle.

CB-13 inhibits HVA-I_{Ca} in small-diameter DRG neurones

We examined the ionic mechanisms that contribute to pain inhibition by CB-13. Under voltage-clamp conditions, bath application of CB-13 (1, 3, and 10 nM) inhibited HVA-I_{Ca} in small-diameter neurones of WT mice (Fig. 4a; $F_{324,1296}=6.42$, $P<0.0001$, two-way mixed-model ANOVA) in a concentration-dependent manner. Increasing CB-13 concentration also progressively decreased HVA-I_{Ca} conductance (Fig. 4b; 1 nM: $t_{132}=3.38$, $P<0.01$; 3 nM: $t_{132}=4.21$, $P<0.001$; 10 nM: $t_{132}=9.67$, $P<0.0001$, Holm–Sidak post-tests). Concentration–effect analysis was performed for peak inhibition at each concentration, with an EC_{50} value of 2.9 nM (Fig. 4c; $R^2=0.79$).

CB-13 inhibition of HVA-I_{Ca} is attenuated by a CB_1R-selective antagonist

We investigated the involvement of CB_1R in inhibition of HVA-I_{Ca} by CB-13. CB-13 (10 nM) induced prolonged inhibition of HVA-I_{Ca}, but the drug effect was attenuated in the presence of AM6545 (10 nM, a CB_1R-selective antagonist, Fig. 5a; $t_{10}=5.5$, $P<0.001$, Holm–Sidak post-test).

Analysis of the I–V relationship showed that CB-13 reduced mean HVA-I_{Ca} conductance (Fig. 5b; $t_{19}=9.7$, $P<0.0001$, Holm–Sidak post-test) and that this effect was decreased by co-application of AM6545 (Fig. 5b; $t_{19}=6.05$, $P<0.0001$, Holm–Sidak post-test). Total HVA-I_{Ca} conductance across all test voltages was calculated by measuring the area under the curve (AUC): CB-13 decreased the AUC from pre-drug values (Fig. 5c; $t_{16}=16.21$, $P<0.0001$, Holm–Sidak post-test), and AM6545 attenuated the CB-13 effect (Fig. 5c; $t_{16}=10.40$, $P<0.0001$, Holm–Sidak post-test). A comparison of inhibition of HVA-I_{Ca} by CB-13 with and without AM6545 is shown in Fig. 5d ($t_8=9.57$, $P<0.0001$, unpaired *t*-test).

CB-13 caused a rightward shift of the open probability curve (Fig. 5e; $t_{187}=2.59$, $P<0.05$), but this effect was blocked in the presence of AM6545 ($t_{187}=1.95$, $P>0.05$, Holm–Sidak post-test).

CB-13 inhibition of HVA-I_{Ca} is reduced in CB_1R conditional knockout mice

AM6545 did not completely block CB-13-induced inhibition of HVA-I_{Ca}, as the remaining HVA-I_{Ca} after co-application of AM6545 and CB-13 was still less than the pre-drug value

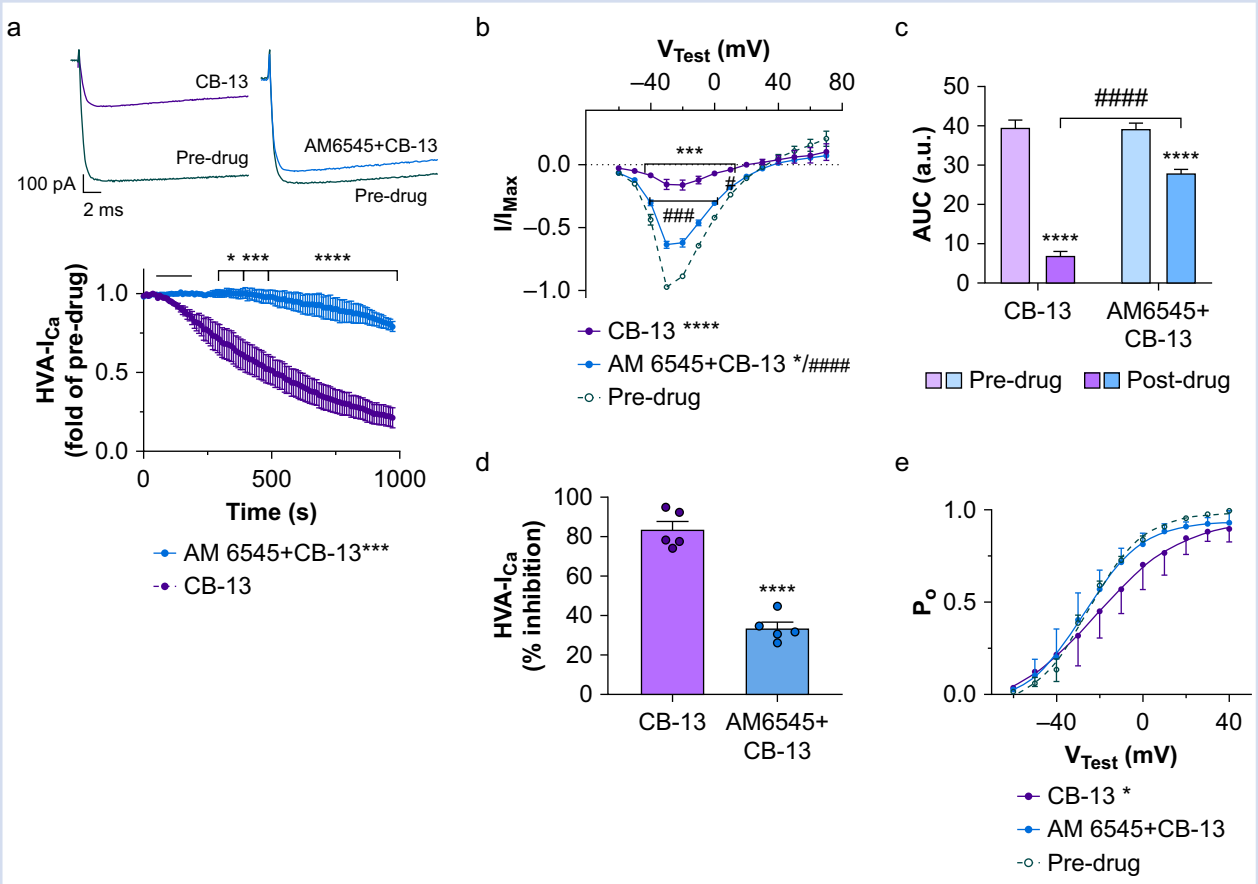

Fig 5. AM6545 significantly attenuates the inhibition of high-voltage activated calcium currents (HVA-I_{Ca}) by CB-13 in small-diameter dorsal root ganglion (DRG) neurones from wild-type (WT) mice. (a) Upper: representative traces of HVA-I_{Ca} in cultured WT DRG neurones under voltage-clamp conditions before and after bath application of 10 nM CB-13 (left) or a combination of 10 nM AM6545 (a selective peripheral CB1R antagonist) and 10 nM CB-13 (right). Lower: time courses of decreased HVA-I_{Ca} after bath application (horizontal black bar) of indicated drug ($F_{216,1080}$=8.19, P<0.0001, two-way repeated measures ANOVA). n=5 neurones/group; *P<0.05, ***P<0.001, ****P<0.0001 *vs* CB-13, Holm–Sidak post-test. (b) The current–voltage (IV) relationship of HVA-I_{Ca} conductance before and after drug treatment ($F_{26,247}$=23.56, P<0.0001, two-way repeated-measures analysis of variance (ANOVA), n=5 neurones/group). CB-13 (****P<0.0001, Holm–Sidak post-test) and AM6545 + CB-13 (t_{19}=2.51, *P<0.05, Holm–Sidak post-test) significantly reduced overall HVA-I_{Ca} conductance. AM6545 significantly reduced the CB-13-induced HVA-ICa inhibition (####P<0.0001, Holm–Sidak post-test, mean effect of AM6545 + CB-13 *vs* CB-13). ***P<0.001 pre-drug *vs* CB-13 at corresponding test voltages; ###P<0.001 for AM6545 + CB-13 *vs* CB-13 at corresponding test voltages, Holm–Sidak post-tests. (c) The areas under the curve (AUC; from V_{Test}=−70 to +40 mV) of I–V relationship before and after drug treatment ($F_{1,16}$=55.78, P<0.0001 *vs* individual pre-drug values, two-way ANOVA, n=5 neurones/group). ****P<0.0001 *vs* pre-drug, ####P<0.0001 *vs* CB-13 post-drug, Holm–Sidak post-test. (d) The overall HVA-I_{Ca} inhibition (% reduction from predrug; I/I_{Max} values at V_{Test}=−30 mV) by CB-13 or AM6545 + CB-13 application. The percent HVA-I_{Ca} inhibition produced by CB-13 application was significantly decreased in the presence of AM6545 (****P<0.0001, unpaired t-test, n=5 neurones/group). (e) Analysis of open probability (PO) curves before and after drug treatment ($F_{2,187}$=3.51, P=0.032, two-way ANOVA, n=5 neurones/group). CB-13 application caused a significant rightward shift of the PO curve (*P<0.05, Holm–Sidak post-test). Co-application of AM6545 and CB-13 did not affect the PO curve (P>0.05, Holm–Sidak post-test). a.u., arbitrary units. (c, f) Pre-drug data were pooled from both groups. Data are shown as mean (standard error of the mean).

(Fig. 5c). It may be that the concentration of AM6545 was insufficient to block CB_1R completely or that CB-13 inhibits HVA-I_{Ca} through targets other than CB_1R. To further examine the influences of CB_1R, and potential CB_2R signalling, on HVA-I_{Ca} inhibition by CB-13, we tested CB-13 along with AM630 (an inverse CB_2R agonist) in small-diameter neurones from CB_1R cKO mice. Both I–V relationship (Fig. 6a) and AUC analysis (Fig. 6b) showed that CB-13 (10 nM) reduced HVA-I_{Ca} from pre-drug levels in CB_1R cKO mice (Fig. 6a; t_{266}=4.48, P<0.0001) without changing the open probability curve (Fig. 6c; t_{209}=1.25, P>0.05, Holm–Sidak post-test). Furthermore, co-application of AM630 did not attenuate CB-13-induced HVA-I_{Ca} inhibition (Fig. 6a; t_{266}=0.832, P>0.05, Holm–Sidak post-test). Changes in AUC were used to compare CB-13-induced inhibition between WT and CB_1R cKO mice. Although CB-13 reduced the AUC in both genotypes (Fig. 6d; t_{24}=17.6, P<0.0001), the effect was less in the cKO group (Fig. 6d; t_{24}=24, P<0.0001, Holm–Sidak post-test). The percent HVA-I_{Ca} inhibition by CB-13 was also lower in cKO than in WT neurones (Fig. 6e; t_{10}=5.37, P=0.0003, unpaired t-test).

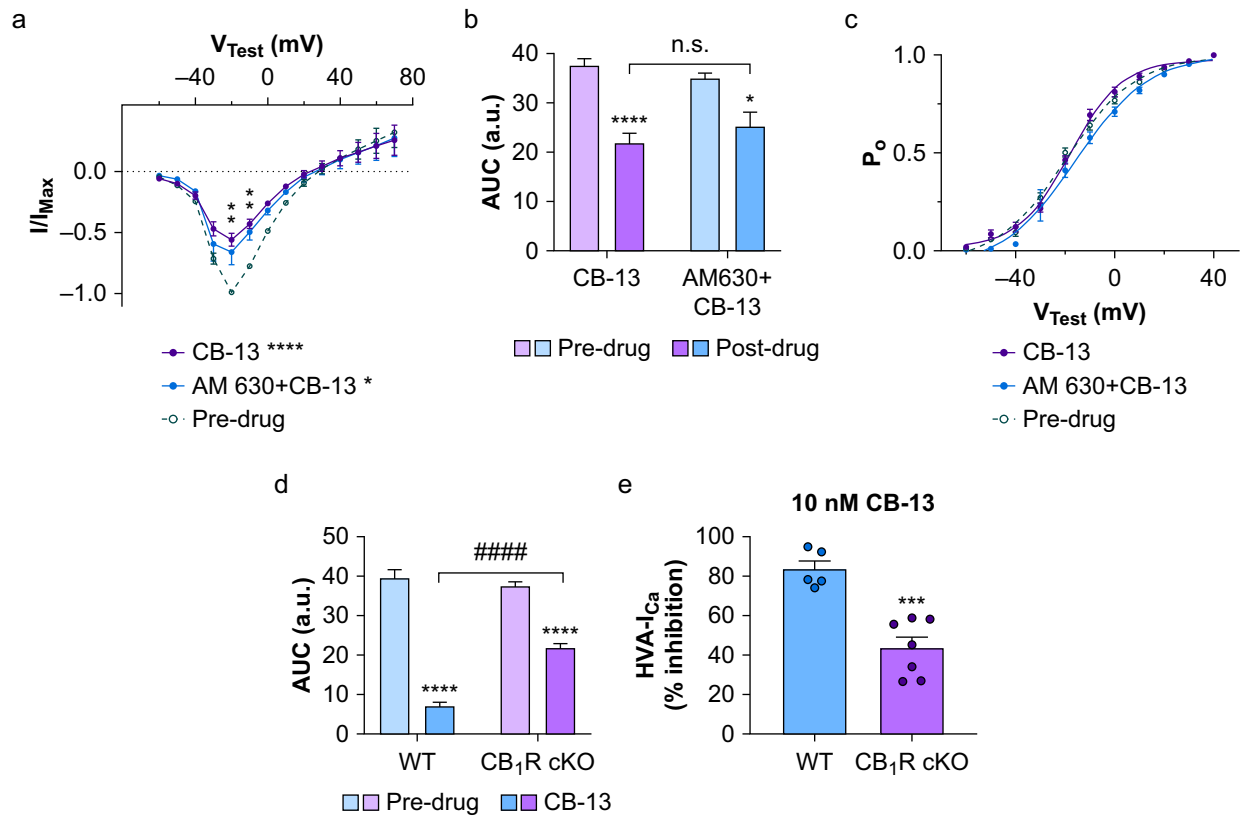

Fig 6. CB-13-induced inhibition of high-voltage activated calcium currents (HVA-I_{Ca}) is attenuated in CB1R conditional knockout (cKO) mice. (a) The current–voltage (I–V) relationships of HVA-I_{Ca} conductance in small-diameter dorsal root ganglion (DRG) neurones from CB1R cKO mice before and after bath application of CB-13 (10 nM, n=7 neurones) or a combination of AM630 (a CB2R inverse agonist, 10 nM) and CB-13 (10 nM, n=4 neurones, $F_{26,266}$=1.94, P=0.0052, two-way mixed-model analysis of variance [ANOVA]). CB-13 application significantly reduced HVA-I_{Ca} conductance (****P<0.0001, Holm–Sidak post-test). Co-application of AM630 and CB-13 induced a similar reduction in HVA-I_{Ca} (t_{266}=2.82, *P<0.05, Holm–Sidak post-test). **P<0.01, CB-13 alone and AM630 + CB-13 *vs* pre-drug at corresponding test voltages, Holm–Sidak post-tests. Pre-drug data were pooled from both groups. (b) The area under the curve (AUC; from V_{Test}=−70 to +40 mV) of the HVA-I_{Ca} I–V relationship before and after drug treatment ($F_{1,18}$=43.17, P<0.0001, two-way ANOVA). *P<0.05, ****P<0.0001 *vs* pre-drug, Holm–Sidak post-test. n.s., not significant. (c) Open probability (Po) curves before and after drug treatment. Application of neither CB-13 nor AM630 + CB-13 altered the Po curve ($F_{20,209}$=1.32, P=0.17, two-way mixed model ANOVA) in CB1R cKO neurones. (d) Comparisons of AUC (from V_{Test}=70 to +40 mV) for the HVA-I_{Ca} I–V relationship before and after CB-13 application in wild-type (WT) and CB1R cKO neurones. CB-13 (10 nM) application still induced a significant reduction of AUC in the CB1R cKO group ($F_{1,24}$=42.02, P<0.0001, two-way mixed-model ANOVA), but the effect was significantly less than that in WT mice. ****P<0.0001 *vs* pre-drug; ####P<0.0001 for comparison of the effect of CB-13 on WT and CB1R cKO neurones, Holm–Sidak post-test. a.u., arbitrary units. (e) Comparison of the overall inhibition of HVA-I_{Ca} (% reduction from pre-drug; I/I_{Max} values at V_{Test}=−20 mV) by CB-13 (10 nM) in WT and CB1R cKO groups. The percent HVA-I_{Ca} inhibition produced by CB-13 was significantly less in CB1R cKO neurones than in WT neurones (***P<0.001, unpaired t-test, n=5 neurones/group).

Discussion

We found that selective deletion of CB_1R in most primary sensory neurones does not affect basal nociceptive thresholds, inflammatory heat hyperalgesia, or intrinsic excitability of small-diameter DRG neurones in mice. However, deletion of CB_1R abolishes the analgesic effects of CB-13 in naïve and inflammatory states and attenuates inhibition of HVA-I_{Ca} by CB-13.

Role of peripheral CB_1R signalling in nociception and inflammatory pain

The endocannabinoid system represents an important component of pain modulatory mechanisms.[32] Mounting evidence suggests that endocannabinoids are important for pain modulation across multiple species.[33–36] CB_1R expression has been localised to DRG neurones in rats, canines, and equines.[33–35] The localisation and function of cannabinoid receptors have also been demonstrated in human sensory neurones.[36] Collectively, these findings suggest that new insights into the endocannabinoid system from studies performed in model species could have high translational impact. Yet, evidence regarding the influence of endogenous CB_1R signalling on pain has been conflicting.[14,16] Global CB_1R KO mice showed either unaltered[37] or decreased pain sensitivity (hypoalgesia) in hot plate assays and formalin tests.[15] Furthermore, functional knockout of CB_1R did not affect the duration or severity of

mechanical hypersensitivity in nerve-injured mice.[38] However, $Na_v1.8$-Cre-driven CB_1R cKO mice exhibited increased basal nociceptive sensitivity, exaggerated inflammatory pain, and elevated excitability in nociceptive afferents, suggesting tonic pain inhibition mediated by CB_1R signalling in nociceptive DRG neurones.[13] In the current study, neither nociceptive thresholds nor inflammatory heat hyperalgesia was altered in *Pirt*-CB_1R cKO mice. After removing an outlier in the cKO group of the hot plate test (Fig. 1h; $P<0.05$; Grubbs test), the comparison is even more similar. Consistent with the behavioural results, electrophysiological recordings showed similar intrinsic excitability in small-diameter DRG neurones of WT and *Pirt*-CB_1R cKO mice when we compared multiple parameters, including resting membrane potential, rheobase level, AP threshold, rate of spontaneous APs, and evoked AP trains.

Multiple factors that require further investigation may explain the discrepancy between our findings and reports in the literature. Previous studies showed that CB_1R mRNA and protein are abundantly expressed in a major subpopulation of nociceptive DRG neurones, but they are also detected in medium- and large-diameter neurones.[12,13,39] Consistent with these findings, we found that CB_1R immunoreactivity was distributed in all sizes of DRG neurones, but the signal was predominant in small-diameter neurones that signal pain and thermal stimuli. Because *Pirt* is expressed in >80% of DRG neurones, but not in the CNS or other cell types in the peripheral nervous system,[17] CB_1R immunoreactivity was substantially decreased across a broad range of DRG neurones in *Pirt*-CB_1R cKO mice. However, it was preserved in large-diameter neurones of $Na_v1.8$-Cre-driven CB_1R cKO mice.[13] Thus, it is plausible that conditionally deleting CB_1R from a subpopulation of nociceptive neurones (with $Na_v1.8$-Cre) and knocking out a much larger population of CB_1R using *Pirt*-Cre may produce different functional changes.

The levels of CB_2R protein were also reduced in the DRGs of CB_1R cKO mice, likely resulting from a loss of membrane stabilisation of CB_2Rs, as G protein-coupled receptors (GPCRs) are known to form heteromers that could modulate the trafficking and post-endocytotic sorting of GPCRs.[40,41] Thus, CB_1 and CB_2 receptors form functional heteromers in the brain, and would likely be subject to altered trafficking or membrane sorting owing to dimerisation.[42] We cannot rule out possible compensatory changes in other receptors, ion channels, and intracellular signalling that may occur and differentially affect pain behaviour in different CB_1R cKO lines. However, *Pirt*-Cre has been used to delete or modulate gene expression selectively in primary sensory neurones without inducing notable compensatory changes.[24,43]

In a previous study,[13] the background genetics of the CB_1 floxed mice consisted of both C57BL/6J and C57BL/6N. Evaluations of these two strains have revealed various phenotypic differences involving metabolism, immunological function, and neurological function.[44] Although it is difficult to attribute the conflicting results to any specific phenotypic difference between the two strains without conducting additional studies, differences in genetic background may introduce variability in pain behaviour tests. In fact, $Na_v1.8$-Cre mice (C57BL/6J background) and $Na_v1.8$-CB_1R cKO mice showed comparable nociceptive thresholds,[13] consistent with our findings that Cre-dependent deletion of CB_1R from DRG neurones does not alter nociceptive thresholds and inflammatory heat hyperalgesia.

CB_1R expression was elevated in DRG and in nerve fibres of skin after CFA-induced inflammation.[39] Although our findings suggest that this increase does not induce tonic CB_1R-mediated pain inhibition, it could increase the efficacy of pain inhibition by exogenous CB_1R agonists.[39] Our data do not exclude the possibility that peripheral endogenous CB_1R signalling controls exaggerated pain in other modalities (e.g. cold, mechanical, ongoing pain) and neurone hyperexcitability after injury. The roles for peripheral CB_1R-mediated signalling in endogenous pain modulation warrant additional investigation, especially to determine whether signalling is context-dependent (e.g. nerve injury, insult severity, post-injury time).

Role of peripheral CB_1R in pain inhibition by CB-13

CB-13 is a CB_1/CB_2R dual agonist with limited CNS penetration. In our behavioural study, systemic administration of CB-13 induced heat and mechanical anti-nociception in naïve WT mice, and attenuated heat hyperalgesia in those with CFA-induced inflammation of the hind paw. The drug effect was diminished in CB_1R cKO mice, suggesting an indispensable role for CB_1R in DRG neurones. These results are in line with previous findings that CB_1R-mediated inhibitory mechanisms in DRG neurones are paramount to the analgesic effects of cannabinoids administrated peripherally[45,46] or systemically.[13]

Inhibition of inflammatory heat hypersensitivity remained significant in *Pirt*-CB_1R cKO at 60 min after systemic CB-13 administration. The remaining effect may be attributable to an incomplete deletion of CB_1R in all DRG neurones, or CB-13 may activate CB_1R expressed in non-neuronal cells (e.g. macrophages, keratinocytes) or other receptors in the peripheral nervous system. Although we cannot completely discount the possibility that some CB-13 may penetrate into the CNS and induce pain inhibition, our results show that acute systemic administration of CB-13 did not alter locomotive activity in open field tests or fall latencies in rotarod tests, which suggests that the dose used in our studies does not have central effects that could alter performance in these assays. Functional interaction between the cannabinoid and opioid systems may participate in pain control.[30,31] However, systemic CB-13-induced pain inhibition remained intact in peripheral MOR cKO mice, suggesting that CB-13 effects were not dependent on MORs in DRG neurones.

Ionic mechanisms involved in CB-13-induced pain inhibition

The cannabinoid agonist WIN55,212-2 inhibits HVA-I_{Ca} in retinal ganglion cells, an effect that was reduced by the CB_1R antagonist SR141716A.[20] We show that CB-13 can concentration-dependently inhibit HVA-I_{Ca} in small-diameter DRG neurones of WT mice, as indicated by decreased current and a rightward shift of the channel open probability curve. This action was reduced in the presence of CB_1R antagonist AM6545 and by CB_1R cKO. HVA calcium channels are important for neurotransmitter release and neuronal excitability,[47] and inhibition of HVA-I_{Ca} contributes to pain inhibition by known analgesics such as morphine and gabapentin.[24,48] Accordingly, pain inhibition by CB-13 may be partially mediated by HVA-I_{Ca} inhibition, which can reduce neurone excitability and nociceptive afferent output.[29,47]

The ability of a CB_1R antagonist and CB_1R cKO to block CB-13-induced HVA-I_{Ca} inhibition was only partial. It is conceivable that other targets on DRG neurones also contribute to the drug effect. CB-13 can activate CB_2R, which is expressed in both rodent and human DRG neurones and plays a functional role in pain.[34,49] Yet the CB_2R-biased inverse agonist AM630 did not attenuate HVA-I_{Ca} inhibition by CB-13 in CB_1R cKO neurones. In addition, CB_2R expression was reduced in the DRGs of CB_1R cKO mice. Taken together, these findings suggest that compensatory changes in CB_2R expression do not underlie HVA inhibition by CB-13 in CB_1R cKO neurones. Further studies are needed to determine if CB-13 has off-target effects on other receptors (e.g. opioid receptors, gamma-aminobutyric acid B [$GABA_B$] receptors) that might also inhibit HVA-I_{Ca}.[24,50,51] Mounting evidence suggests that cannabinoids have both metabotropic and ionotropic receptor targets that contribute to the modulation of pain processing,[21] including voltage-gated calcium channels, potassium channels, diverse transient receptor potential channels (e.g. TRPV1), acid-sensing ion channels, and purinergic receptors (e.g. P2X3).[21–23,52] Thus, the complete underlying ionic mechanisms and molecular targets responsible for CB-13-induced neuronal and pain inhibition warrant further investigation.

Conclusions

By a combination of genetic, behavioural, pharmacological, and electrophysiological approaches, we show that CB_1R in mouse DRG neurones is essential to mediating the analgesic effects of systemic CB-13, and that HVA-I_{Ca} inhibition is a potential ionic mechanism for CB-13-induced analgesia. However, peripheral CB_1R-mediated signalling may not tonically inhibit nociceptive thresholds or inflammatory heat hyperalgesia, nor affect the intrinsic excitability of nociceptive DRG neurones in mice. These findings contribute to our understanding of how CB_1Rs expressed in primary sensory neurones affect pain and cannabinoid analgesia. CB_1R activation in the brain causes myriad side-effects that significantly limit CB_1R agonist use, but our study suggests that peripherally acting CB_1R agonists may have potential for pain management.

Authors' contributions

Study design: SR, YG, NCF, QH, AB
Experimental design for conditional knockout species: XD
Conduct of most of the experiments: NCF, AB
Conduct of portions of experiments: SH, QH, CZ
Data analysis: NCF, AB, SH, QH, CZ
Discussion of the work: NCF, XD, YG, SR
Directed the project: SR, YG
Drafting of the manuscript: NCF, AB, YG, SR
Manuscript review: SH, QH, CZ
All authors read and approved the final manuscript.

Acknowledgements

The authors thank Claire Gaveriaux-Ruff (University of Strasbourg, France), George Kunos (US National Institutes of Health, Bethesda, MD, USA), and Elisabeth Glowatzki (Johns Hopkins University School of Medicine, Baltimore, MD, USA) for providing the transgenic mice. The authors also thank Claire Levine (Department of Anesthesiology and Critical Care Medicine, Johns Hopkins University) for assistance in editing the manuscript.

Declarations of interest

SNR is a consultant for Allergan, Averitas Pharma, Bayer, and Lexicon Pharmaceuticals, and has consulted for Aptinyx Inc., Heron Therapeutics, and Insys Therapeutics. YG and SNR are principal and co-investigators in a research grant from Medtronic, Inc. YG received a research award from TissueTech, Inc. The other authors declare no other potential conflicts of interest with respect to the research, authorship, and/or publication of this article.

Funding

National Institutes of Health (Bethesda, MD, USA) (NS026363 to SNR; NS110598, NS117761, and NS070814 to YG; NS070201 [NINDS T32] to NCF). This work was facilitated by the Pain Research Core funded by the Blaustein Fund and the Neurosurgery Pain Research Institute at the Johns Hopkins University (Baltimore, MD, USA).

Appendix A. Supplementary data

Supplementary data to this article can be found online at https://doi.org/10.1016/j.bja.2021.10.020.

References

1. Naim MM, Shehab SA, Todd AJ. Cells in laminae III and IV of the rat spinal cord which possess the neurokinin-1 receptor receive monosynaptic input from myelinated primary afferents. *Eur J Neurosci* 1998; **10**: 3012–9
2. Light AR, Perl ER. Spinal termination of functionally identified primary afferent neurons with slowly conducting myelinated fibers. *J Comp Neurol* 1979; **186**: 133–50
3. Johannes CB, Le TK, Zhou X, Johnston JA, Dworkin RH. The prevalence of chronic pain in United States adults: results of an Internet-based survey. *J Pain* 2010; **11**: 1230–9
4. Fayaz A, Croft P, Langford RM, Donaldson LJ, Jones GT. Prevalence of chronic pain in the UK: a systematic review and meta-analysis of population studies. *BMJ Open* 2016; **6**, e010364
5. Gaskin DJ, Richard P. The economic costs of pain in the United States. *J Pain* 2012; **13**: 715–24
6. Breivik H, Eisenberg E, O'Brien T. Openminds. The individual and societal burden of chronic pain in Europe: the case for strategic prioritisation and action to improve knowledge and availability of appropriate care. *BMC Public Health* 2013; **13**: 1229
7. Gregorian Jr RS, Gasik A, Kwong WJ, Voeller S, Kavanagh S. Importance of side effects in opioid treatment: a trade-off analysis with patients and physicians. *J Pain* 2010; **11**: 1095–108
8. Boudreau D, Von Korff M, Rutter CM, et al. Trends in long-term opioid therapy for chronic non-cancer pain. *Pharmacoepidemiol Drug Saf* 2009; **18**: 1166–75
9. Pacher P, Batkai S, Kunos G. The endocannabinoid system as an emerging target of pharmacotherapy. *Pharmacol Rev* 2006; **58**: 389–462
10. Dziadulewicz EK, Bevan SJ, Brain CT, et al. Naphthalen-1-yl-(4-pentyloxynaphthalen-1-yl)methanone: a potent,

orally bioavailable human CB1/CB2 dual agonist with antihyperalgesic properties and restricted central nervous system penetration. *J Med Chem* 2007; **50**: 3851–6
11. Salio C, Fischer J, Franzoni MF, Conrath M. Pre- and postsynaptic localizations of the CB1 cannabinoid receptor in the dorsal horn of the rat spinal cord. *Neuroscience* 2002; **110**: 755–64
12. Mitrirattanakul S, Ramakul N, Guerrero AV, et al. Site-specific increases in peripheral cannabinoid receptors and their endogenous ligands in a model of neuropathic pain. *Pain* 2006; **126**: 102–14
13. Agarwal N, Pacher P, Tegeder I, et al. Cannabinoids mediate analgesia largely via peripheral type 1 cannabinoid receptors in nociceptors. *Nat Neurosci* 2007; **10**: 870–9
14. Richardson JD, Aanonsen L, Hargreaves KM. SR 141716A, a cannabinoid receptor antagonist, produces hyperalgesia in untreated mice. *Eur J Pharmacol* 1997; **319**: R3–4
15. Zimmer A, Zimmer AM, Hohmann AG, Herkenham M, Bonner TI. Increased mortality, hypoactivity, and hypoalgesia in cannabinoid CB1 receptor knockout mice. *Proc Natl Acad Sci U S A* 1999; **96**: 5780–5
16. Beaulieu P, Bisogno T, Punwar S, et al. Role of the endogenous cannabinoid system in the formalin test of persistent pain in the rat. *Eur J Pharmacol* 2000; **396**: 85–92
17. Kim AY, Tang Z, Liu Q, et al. Pirt, a phosphoinositide-binding protein, functions as a regulatory subunit of TRPV1. *Cell* 2008; **133**: 475–85
18. Walker JM, Huang SM. Cannabinoid analgesia. *Pharmacol Ther* 2002; **95**: 127–35
19. Berrocoso E, Rey-Brea R, Fernandez-Arevalo M, Mico JA, Martin-Banderas L. Single oral dose of cannabinoid derivate loaded PLGA nanocarriers relieves neuropathic pain for eleven days. *Nanomedicine* 2017; **13**: 2623–32
20. Ross RA, Coutts AA, McFarlane SM, et al. Actions of cannabinoid receptor ligands on rat cultured sensory neurones: implications for antinociception. *Neuropharmacology* 2001; **40**: 221–32
21. Akopian AN, Ruparel NB, Jeske NA, Patwardhan A, Hargreaves KM. Role of ionotropic cannabinoid receptors in peripheral antinociception and antihyperalgesia. *Trends Pharmacol Sci* 2009; **30**: 79–84
22. Liu YQ, Qiu F, Qiu CY, et al. Cannabinoids inhibit acid-sensing ion channel currents in rat dorsal root ganglion neurons. *PLoS One* 2012; **7**, e45531
23. Mackie K, Lai Y, Westenbroek R, Mitchell R. Cannabinoids activate an inwardly rectifying potassium conductance and inhibit Q-type calcium currents in AtT20 cells transfected with rat brain cannabinoid receptor. *J Neurosci* 1995; **15**: 6552–61
24. Barpujari A, Ford N, He SQ, et al. Role of peripheral sensory neuron mu-opioid receptors in nociceptive, inflammatory, and neuropathic pain. *Reg Anesth Pain Med* 2020; **45**: 907–16
25. Liu S, Huang Q, He S, et al. Dermorphin [D-Arg2, Lys4] (1–4) amide inhibits below-level heat hypersensitivity in mice after contusive thoracic spinal cord injury. *Pain* 2019; **160**: 2710–23
26. Tiwari V, Anderson M, Yang F, et al. Peripherally acting mu-opioid receptor agonists attenuate ongoing pain-associated behavior and spontaneous neuronal activity after nerve injury in rats. *Anesthesiology* 2018; **128**: 1220–36
27. Guan Y, Liu Q, Tang Z, Raja SN, Anderson DJ, Dong X. Mas-related G-protein-coupled receptors inhibit pathological pain in mice. *Proc Natl Acad Sci U S A* 2010; **107**: 15933–8
28. Chen H, Ikeda SR. Modulation of ion channels and synaptic transmission by a human sensory neuron-specific G-protein-coupled receptor, SNSR4/mrgX1, heterologously expressed in cultured rat neurons. *J Neurosci* 2004; **24**: 5044–53
29. Li Z, Tseng PY, Tiwari V, et al. Targeting human Mas-related G protein-coupled receptor X1 to inhibit persistent pain. *Proc Natl Acad Sci U S A* 2017; **114**: E1996–2005
30. Desroches J, Bouchard JF, Gendron L, Beaulieu P. Involvement of cannabinoid receptors in peripheral and spinal morphine analgesia. *Neuroscience* 2014; **261**: 23–42
31. Mohammadkhani A, Borgland SL. Cellular and behavioral basis of cannabinioid and opioid interactions: implications for opioid dependence and withdrawal. *J Neurosci Res* 2020. https://doi.org/10.1002/jnr.24770
32. Woodhams SG, Chapman V, Finn DP, Hohmann AG, Neugebauer V. The cannabinoid system and pain. *Neuropharmacology* 2017; **124**: 105–20
33. Ahluwalia J, Urban L, Capogna M, Bevan S, Nagy I. Cannabinoid 1 receptors are expressed in nociceptive primary sensory neurons. *Neuroscience* 2000; **100**: 685–8
34. Chiocchetti R, Galiazzo G, Tagliavia C, et al. Cellular distribution of canonical and putative cannabinoid receptors in canine cervical dorsal root ganglia. *Front Vet Sci* 2019; **6**: 313
35. Chiocchetti R, Rinnovati R, Tagliavia C, et al. Localisation of cannabinoid and cannabinoid-related receptors in the equine dorsal root ganglia. *Equine Vet J* 2021; **53**: 549–57
36. Anand U, Otto WR, Sanchez-Herrera D, et al. Cannabinoid receptor CB2 localisation and agonist-mediated inhibition of capsaicin responses in human sensory neurons. *Pain* 2008; **138**: 667–80
37. Ledent C, Valverde O, Cossu G, et al. Unresponsiveness to cannabinoids and reduced addictive effects of opiates in CB1 receptor knockout mice. *Science* 1999; **283**: 401–4
38. Wilkerson JL, Alberti LB, Kerwin AA, et al. Peripheral versus central mechanisms of the cannabinoid type 2 receptor agonist AM1710 in a mouse model of neuropathic pain. *Brain Behav* 2020; **10**, e01850
39. Amaya F, Shimosato G, Kawasaki Y, et al. Induction of CB1 cannabinoid receptor by inflammation in primary afferent neurons facilitates antihyperalgesic effect of peripheral CB1 agonist. *Pain* 2006; **124**: 175–83
40. Gurevich VV, Gurevich EV. GPCR monomers and oligomers: it takes all kinds. *Trends Neurosci* 2008; **31**: 74–81
41. He SQ, Zhang ZN, Guan JS, et al. Facilitation of mu-opioid receptor activity by preventing delta-opioid receptor-mediated codegradation. *Neuron* 2011; **69**: 120–31
42. Callen L, Moreno E, Barroso-Chinea P, et al. Cannabinoid receptors CB1 and CB2 form functional heteromers in brain. *J Biol Chem* 2012; **287**: 20851–65
43. Gao X, Han S, Huang Q, et al. Calcium imaging in population of dorsal root ganglion neurons unravels novel mechanisms of visceral pain sensitization and referred somatic hypersensitivity. *Pain* 2021; **162**: 1068–81
44. Simon MM, Greenaway S, White JK, et al. A comparative phenotypic and genomic analysis of C57BL/6J and C57BL/6N mouse strains. *Genome Biol* 2013; **14**: R82
45. Johanek LM, Simone DA. Activation of peripheral cannabinoid receptors attenuates cutaneous hyperalgesia produced by a heat injury. *Pain* 2004; **109**: 432–42
46. Yu XH, Cao CQ, Martino G, et al. A peripherally restricted cannabinoid receptor agonist produces robust anti-nociceptive effects in rodent models of inflammatory and neuropathic pain. *Pain* 2010; **151**: 337–44

47. Hoppa MB, Lana B, Margas W, Dolphin AC, Ryan TA. alpha2delta expression sets presynaptic calcium channel abundance and release probability. *Nature* 2012; **486**: 122–5
48. Callaghan B, Haythornthwaite A, Berecki G, Clark RJ, Craik DJ, Adams DJ. Analgesic alpha-conotoxins Vc1.1 and Rg1A inhibit N-type calcium channels in rat sensory neurons via GABAB receptor activation. *J Neurosci* 2008; **28**: 10943–51
49. Beltramo M, Bernardini N, Bertorelli R, et al. CB2 receptor-mediated antihyperalgesia: possible direct involvement of neural mechanisms. *Eur J Neurosci* 2006; **23**: 1530–8
50. Sadeghi M, Carstens BB, Callaghan BP, et al. Structure-activity studies reveal the molecular basis for GABAB-receptor mediated inhibition of high voltage-activated calcium channels by alpha-conotoxin Vc1.1. *ACS Chem Biol* 2018; **13**: 1577–87
51. Park KS, Jeong SW, Cha SK, et al. Modulation of N-type Ca^{2+} currents by A1-adenosine receptor activation in male rat pelvic ganglion neurons. *J Pharmacol Exp Ther* 2001; **299**: 501–8
52. Oliveira-Fusaro MCG, Zanoni CIS, Dos Santos GG, et al. Antihyperalgesic effect of CB1 receptor activation involves the modulation of P2X3 receptor in the primary afferent neuron. *Eur J Pharmacol* 2017; **798**: 113–21

Handling editor: Hugh C Hemmings Jr